IEEE Photonics Journal
An IEEE Photonics Society Publication

Open Access

High-Stability Broadband Wavelength-Tunable Single-Frequency Ytterbium-Doped All-Fiber Compound Ring Cavity

Volume 9, Number 2, April 2017

Bao-le Lu
Jin Kang
Xin-Yuan Qi
Xiao-Qiang Feng
Lei Hou
Man Jiang
Hao-Wei Chen
Yang Wang
Kai-Le Wang
Jin-Tao Bai

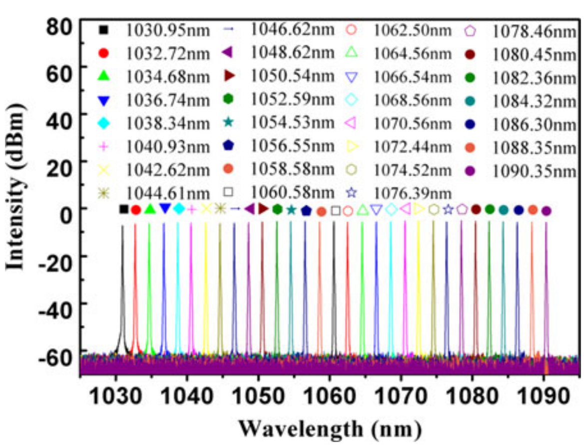

DOI: 10.1109/JPHOT.2017.2657747

High-Stability Broadband Wavelength-Tunable Single-Frequency Ytterbium-Doped All-Fiber Compound Ring Cavity

Bao-le Lu,[1,2,3] Jin Kang,[1,2,3] Xin-Yuan Qi,[1,2,3,4] Xiao-Qiang Feng,[1,2,3] Lei Hou,[1,2,3] Man Jiang,[1,2,3] Hao-Wei Chen,[1,2,3] Yang Wang,[1,2,3] Kai-Le Wang,[1,2,3] and Jin-Tao Bai[1,2,3,4]

[1]National Key Laboratory of Photoelectric Technology and Functional Materials (Culture Base), Institute of Photonics and Photon-Technology, Northwest University, Xi'an 710069, China
[2]Shaanxi Engineering Technology Research Center for Solid State Lasers and Application, Xi'an 710069, China
[3]Institute of Photonics and Photon-Technology, Provincial Key Laboratory of Photo-Electronic Technology, Northwest University, Xi'an 710069, China
[4]School of Physics, Northwest University, Xi'an 710069, China

DOI:10.1109/JPHOT.2017.2657747

Manuscript received November 16, 2016; revised January 9, 2017; accepted January 20, 2017. Date of publication January 25, 2017; date of current version April 5, 2017. This work was supported in part by the National Nature Science Foundation of China under Grant 61475125; in part by the Natural Science Foundation of Shaanxi Province, China, under Grant 2016JM6083 and Grant 2016JQ6059; in part by the Foundation of the Education Committee of Shaanxi Province under Grant 16JK1769 and Grant 14JK1756; and in part by the Science Foundation of Northwest University under Grant 15NW07 and Grant 13NW14. Corresponding authors: X.-Y. Qi and J.-T. Bai (e-mail: qixycn@nwu.edu.cn; baijt@nwu.edu.cn.com).

Abstract: A high-stability wavelength-tunable single-frequency (SF) ytterbium-doped all-fiber compound ring laser has been demonstrated experimentally. The compound ring cavity is composed of a fiber optical tunable filter, a high-finesse ring filter, and a loop mirror filter. Three segments of ytterbium-doped fibers are employed as the gain medium or saturable absorber, respectively. The SF operation is observed to be stable during 1 h without mode hopping. The SF fiber laser achieves a wide-band tunability from 1030 to 1090 nm with maximum output slope efficiency of 7.95%. The power instability over 2 h gives standard deviation value of 1.34%. The average linewidth is 8.8 kHz and the relaxation oscillation frequency is at 62 kHz.

Index Terms: Single frequency fiber laser, wavelength-tunable, high-finesse ring filter, loop mirror filter.

1. Introduction

Single frequency fiber laser sources, due to their excellent monochromaticity, outstanding stability, and coherence, exhibit promising potentials in a large amount of fields such as Doppler LIDAR, gravitational wave detectors, high resolution sensing, optical fiber sensors, and coherent telecommunication over the past few decades [1]–[4]. Over the past several decades, the linear cavity [5]–[9] and the ring cavity [10] have been studied profoundly in the field of SF fiber lasers. Among them, a plenty of works on the SF fiber lasers show that the linear cavity is suitable for the single

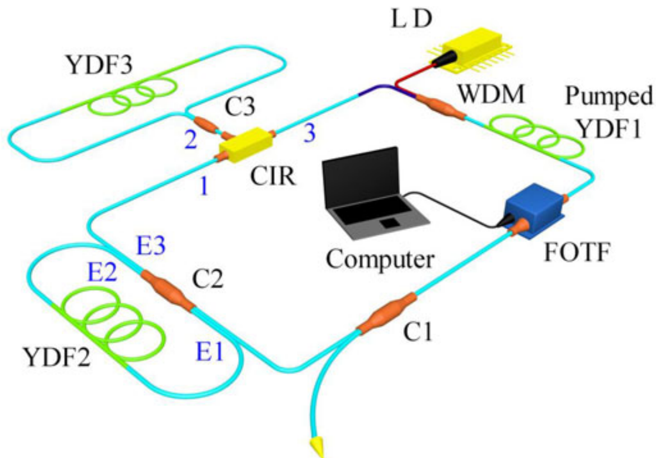

Fig. 1. Schematic of the wavelength-tunable SF ytterbium-doped fiber laser with a compound ring cavity. LD: Laser diode; WDM: Wavelength division multiplexer; YDF: Ytterbium-doped fiber; FOTF: Fiber optical tunable filter; C: Coupler.

wavelength laser [5], [6], rather than the broadband wavelength-tunable operation. The ring cavity, lacking the spatial hole-burning (SHB) effect in a traveling-wave field, is demonstrated to be more suitable for wavelength-tunable SF oscillation than the linear cavity design. Therefore, it attracts more and more attention in recent years. Wavelength-tunable SF fiber lasers with ring cavity have been studied extensively [10]–[14]. Many key techniques are used to realize tunable wavelength SF operation, such as, using a highly stretchable fiber Bragg grating (FBG) and unpumped erbium-doped fiber [11], using cascaded fiber Sagnac loop filters [12], using a compound cavity composed of an active main ring cavity and several passive subring cavities [13], using an integrated silicon-on-insulator micro-ring resonator and two subsidiary fiber rings [14], and using a passive subring cavity [10].

In this paper, we propose a high stability wavelength-tunable SF ytterbium-doped all-fiber compound ring laser. The compound ring cavity is constructed with a FOTF, a HFRF and a LMF. The central wavelength of our SF fiber laser is tuned continuously by the FOTF over a broad wavelength region from 1030 nm to 1090 nm. The maximum output slope efficiency is 7.95%. The power instability over 2 h gives standard deviation value of 1.34%. The average linewidth is 8.8 kHz and the relaxation oscillation frequency is at 62 kHz.

2. Experimental Setup and Principles

The schematic of the wavelength-tunable SF ytterbium-doped all-fiber compound ring laser is illustrated in Fig. 1. The pump laser with maximum power of 650 mW at 975 nm passes through a 980/1060 nm WDM and then is imported into an 80 cm long gain medium YDF1. The spontaneous light emission from YDF1 propagates through a FOTF with central wavelength 3 dB bandwidth of 1 nm and tunable wavelength region of 1020 nm to 1090 nm. A computer is connected with the FOTF through a digital cable to tune the central wavelength. A 20/80 coupler C1 (1×2) is used as the output element. A HFRF consisted of a 3 dB optical coupler C2 (2×2) and an 1.5 m unpumped YDF2, a LMF constructed by a 3 dB coupler C3 (1×2), and a 2 m unpumped YDF3, and a three ports CIR are inserted in turn in the cavity. The core diameters of all the YDFs are 6 μm and the numerical apertures (N. A.) of all the YDFs are equal to 0.13. The concentration of the ytterbium ion is 21,000 ppm (INO Yb 501). All the couplers, which have a wide band to encompass larger tuning range to optimally accommodate fiber laser, are fused tapered in our experiment. Besides, 45 dB isolation from port 3 to port 2, as well as from port 2 to port 1 in the circulator, ensures the unidirectional propagation of the laser and prevents the backward reflections.

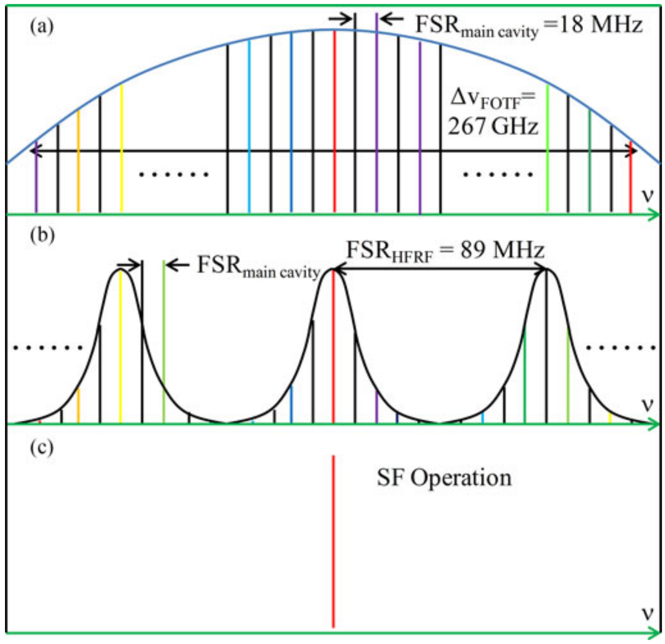

Fig. 2. Mode selection in the proposed fiber laser. (a) With FOTF. (b) With FOTF and HFRF. (c) With FOTF and HFRF and LMF.

In our experimental configuration, the longitudinal mode space of the main cavity is about 18 MHz [see Fig. 2(a)]. To obtain the SF operation, the HFRF and the LMF are the employed. When the input field E1 is injected into the HFRF, light will be divided into E2 and E3 (Fig. 1). The transmission of the HFRF is expressed as [15]

$$T = \frac{(E_2)^2}{(E_1)^2} = \frac{r}{1 + g^2(1 - r) - 2g\sqrt{1 - r}\cos(\tau\omega)} \tag{1}$$

where r is the splitting ratio of coupler C2 (2×2), and g is the gain of YDF2. ω is the angular frequency of the optical fields and τ is the time delay of HFRF ($\tau = 2\pi/FSR$). $FSR = c/n_{eff}l$, where $l = 2.3$ m is the length of the HFRF. The spectral filter response of the HFRF is shown in Fig. 2(b). Clearly it has effectively suppressed a part of the multi-modes around the transmission peak.

When the light passes through the ports 1 and 2 of CIR, two opposite-directional propagating light interference in the unpumped YDF3. According to the theories of standing wave and nonlinear optics, a dynamically periodical distribution of the refractive index forms in the LMF. The dynamic Bragg grating (DBG) works as an ultra-narrow self-tracking filter. Its full width at half-maximum (FWHM) can be calculated as [16]

$$\Delta f = \frac{c}{\lambda}\kappa\sqrt{\left(\frac{\Delta n}{2n_{eff}}\right)^2 + \left(\frac{\lambda}{2n_{eff}L_g}\right)^2}. \tag{2}$$

The coupling coefficient of the induced DBG κ is written as [17]

$$\kappa = \frac{2\Delta n}{n_{eff}\lambda} \tag{3}$$

where λ is the central wavelength, and n is the effective refraction index of the unpumped YDF3. L_g is the length of the DBG. Δn is the variation of the refractive index, which can be given by the well-known Kramers–Kronig relation [15]. In our experiment, $\lambda = 1060$ nm, $L_g = 2$ m, and $n_{\text{eff}} = 1.45$, the change of the refraction index is estimated to be $\Delta n < 2 \times 10^{-7}$, and therefore, the FWHM of

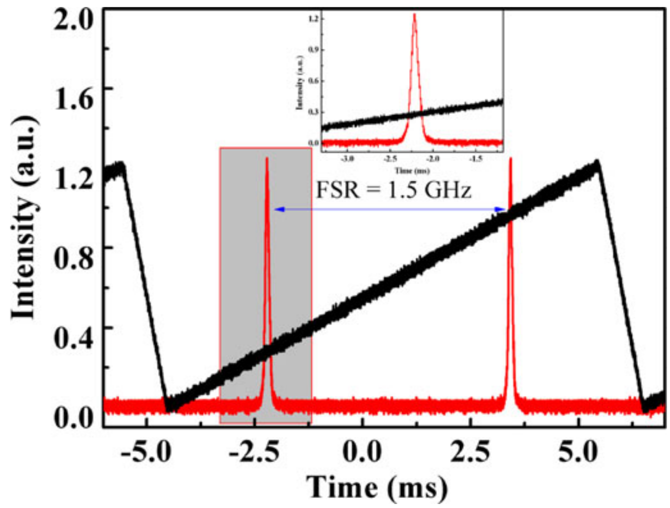

Fig. 3. SF characteristics measured by a scanning F-P interferometer. (Inset) Enlarged signal figure with a smooth lineshape.

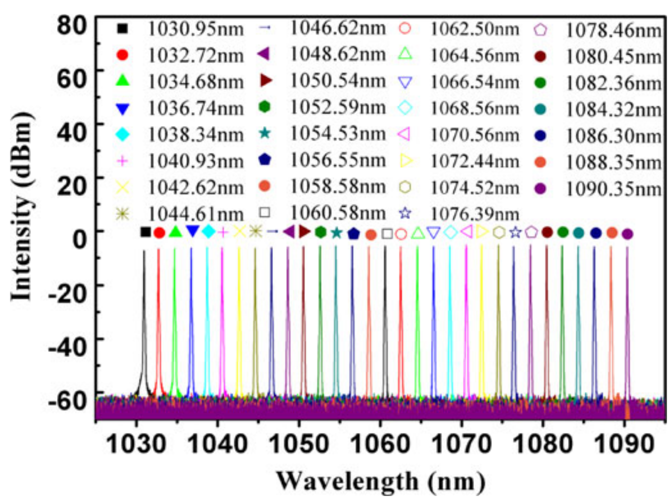

Fig. 4. Output spectra of the proposed SF fiber laser with wavelength tuned from 1030 nm to 1090 nm.

the LMF is about $\Delta f < 14$ MHz, which is smaller than the longitudinal mode space of the main cavity ($FSR_{\text{main cavity}} = 18$ MHz). Fig. 2(c) shows the SF operation spectra of our laser.

3. Experimental Results

Further experimental observations are carried on by a scanning Fabry-Peort (F-P) interferometer (Thorlabs, SA210) and an oscillator (Agilent technologies DSO9104A). The free spectral range (FSR) and the finesse of the interferometer are 1.5 GHz and 200. Fig. 3 shows the curves of the F-P ramp voltage (the black sawtooth wave) and the longitudinal modes of the laser (the red peaks). Apparently, two red peaks distribute exactly in one F-P ramp, demonstrating that the laser achieves SF operation. The inset also shows that the enlarged signal figure has a smooth lineshape, confirming further that the SF fiber laser operates consistently without any other modes and mode competition phenomenon.

By controlling the working wavelength of FOTF through the computer, the central wavelength of the generated SF fiber laser is tuned. Fig. 4 shows the output spectra (Yokogawa, AQ6370C, with

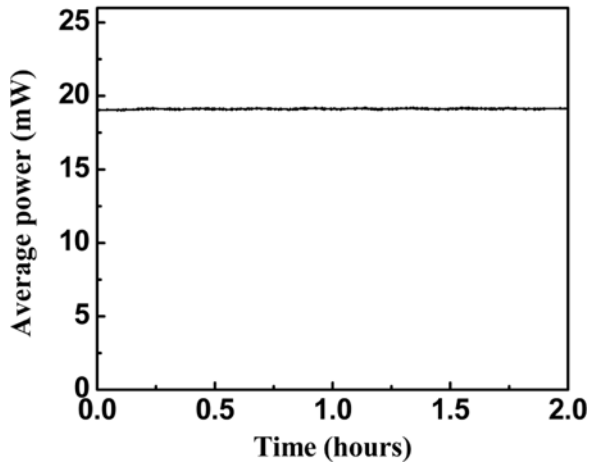

Fig. 5. Observation of the output power stability of the SF fiber laser at 1060.58 nm.

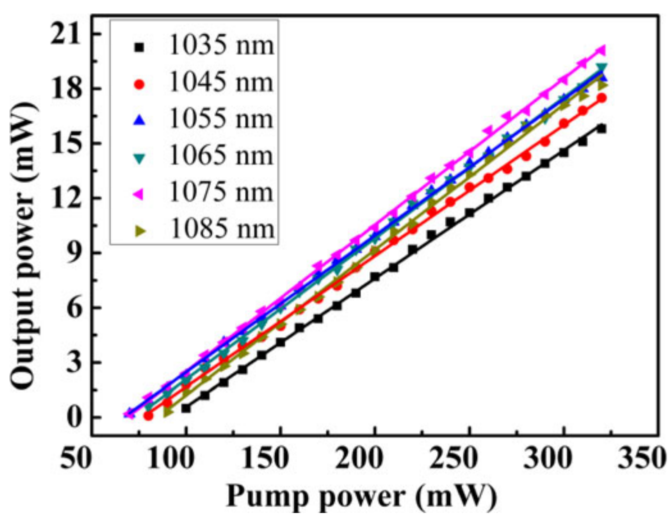

Fig. 6. Curves of the output power versus the pump power at different central wavelengths.

a 0.02 nm resolution) of the SF laser at an interval of 2 nm at a constant pump power of 300 mW. Obviously, the fiber laser obtains SF operation tuned continuously from 1030 nm to 1090 nm. The OSNR is higher than 50 dB and no mode hopping is observed as the wavelengths are tuned.

The stability of the fiber laser is investigated. Fig. 5 shows the average output power at 1060.58 nm from the 20% port of the 20/80 coupler. The instabilities over 2 h give standard deviation value of 1.34%, which indicates an excellent power and the stability of SF fiber laser.

Fig. 6 shows the curves of the SF output power versus the pump power at different central wavelengths. Their corresponding slope efficiencies are 6.89% (@1035 nm), 7.16% (@1045 nm), 7.47% (@1055 nm), 7.74% (@1065 nm), 7.95% (@1075 nm), and 7.78% (@1085 nm), respectively. It is clear that different operation wavelengths have different slope efficiency and different threshold power. The maximum output power of SF fiber laser, 20.1 mW, is obtained at the wavelength of 1075 nm when the pump power is 320 mW. Since the gain coefficient of the ytterbium-doped fiber at the wavelength of 1030 nm is the strongest, it should have the largest the amplification factor, that is the largest slope efficiency. However, our results demonstrate that the amplification factor will be larger when the wavelength is longer. This means that the amplified spontaneous emission

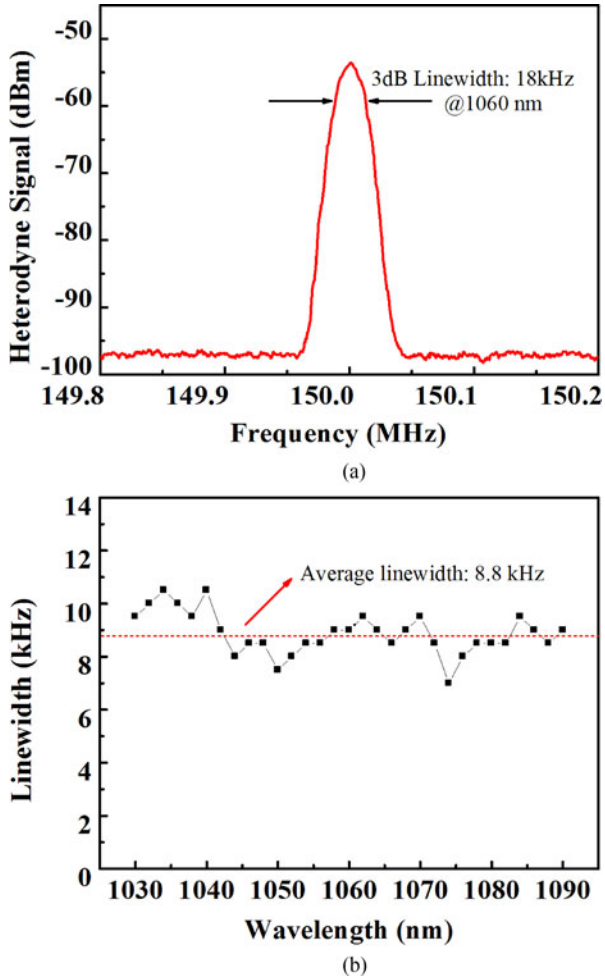

Fig. 7. (a) Measured lineshape of the self-heterodyne signal by using a 30 km delay fiber. (b) Linewidth measurement versus different wavelengths.

at wavelength shorter than the lasing wavelength will be reabsorbed. Note that the laser efficiency is rather low chiefly as a consequence of the high insertion loss of the cavity and output coupler ratio.

The linewidth of the SF fiber laser is measured by the delayed self-heterodyne method using a 30 km single mode delay fiber [18], [19], whose linewidth resolution is around 6.6 kHz. Fig. 7(a) shows the 3 dB linewidth of the SF fiber laser at the central wavelength of 1060 nm. Since the linewidth of the optical spetrum is 1/2 of the 3 dB bandwidth of the self-heterodyne signal curve [18], the linewidth of our output laser with 200 mW pump power is calculated be 9 kHz at 1060 nm. The linewidth measurements for all the 31 tuning wavelengths are shown in Fig. 7(b). The average linewidth is 8.8 kHz. This shows that our tunable laser can achieve a very narrow linewidth output within a very large tunable wavelength range.

The RIN of the SF fiber laser is performed with the RF spectrum analyzer (KEYSIGHT N9000A) and the photodetector (Newport Model-1601) with 3 dB cutoff frequency of 1 GHz. When the pump laser is out off power, the curve of RIN of instrument (Received noise) is obtained as shown in black (Fig. 8). Fig. 8 mainly depicts a peak in the signal spectrum at about 62 kHz, which is the relaxation oscillation frequency of the SF fiber laser in the frequency range from 0 to 1 MHz at the pump power power of 200 mW. The relaxation oscillation stems from the dynamic energy

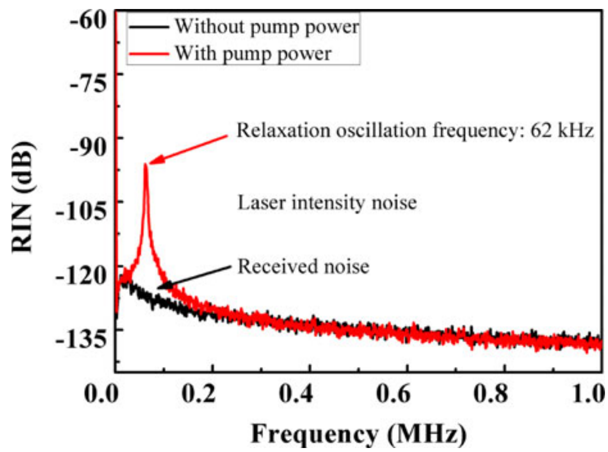

Fig. 8. Relative intensity noise (RIN) spectrum of the SF fiber laser from 0 to 1 MHz. The relaxation oscillation frequency is at 62 kHz.

exchange process between the injected pump field and the laser signal field [20]. Compared with the received noise, there are no additional noise components observed for frequencies above 200 kHz [21].

4. Conclusion

In summary, we propose and experimentally demonstrate a high stability SF ytterbium-doped all-fiber laser with a compound ring cavity. The HFRF and LMF in the cavity guarantee the SF operation. The SF fiber laser achieves a broad-band tunability from 1030 nm to 1090 nm with maximum output slope efficiency of 7.95% by using a FOFT. The average linewidth is about 8.8 kHz. The power instability over 2 h gives standard deviation value of 1.34%. The relaxation oscillation frequency of the SF fiber laser is at about 62 kHz.

References

[1] J. G. Williams, S. G. Turyshev, and D. H. Boggs, "Progress in lunar laser ranging tests of relativistic gravity," *Phys. Rev. Lett.*, vol. 93, no. 26, 2004, Art. no. 261101.

[2] G. J. Ray, T. N. Anderson, J. A. Caton, R. P. Lucht, and T. Walther, "OH sensor based on ultraviolet, continuous-wave absorption spectroscopy utilizing a frequency-quadrupled, fiber-amplified external-cavity diode laser," *Opt. Lett.*, vol. 26, no. 23, pp. 1870–1872, 2002.

[3] R. Su, P. Zhou, X. Wang, H. Zhang, and X. Xu, "Active coherent beam combining of a five-element, 800 W nanosecond fiber amplifier array," *Opt. Lett.*, vol. 37, no. 19, pp. 3978–3980, 2012.

[4] M. Engelbrecht, A. Ruehl, D. Wandt, and D. Kracht, "Single-frequency ytterbium-doped fiber laser with 26 nm tuning range," *Opt. Exp.*, vol. 15, no. 8, pp. 4617–4622, 2007.

[5] X. Huang *et al.*, "Linewidth suppression mechanism of self-injection locked single-frequency fiber laser," *Opt. Exp.*, vol. 24, no. 17, pp. 18907–18916, 2016.

[6] Y. Zhang *et al.*, "Compact frequency-modulation Q-switched single-frequency fiber laser at 1083 nm," *J. Opt.*, vol. 17, no. 12, 2015, Art. no. 125705.

[7] J. Deng *et al.*, "Single frequency Yb-fiber laser based on graphene loop mirror filter," *J. Opt.*, vol. 17, no. 2, 2015, Art. no. 025802.

[8] S. Xu *et al.*, "400 mW ultrashort cavity low-noise single-frequency Yb^{3+}-doped phosphate fiber laser," *Opt. Lett.*, vol. 36, no. 18, pp. 3708–3710, 2011.

[9] S. Xu *et al.*, "Low noise single-frequency single-polarization ytterbium-doped phosphate fiber laser at 1083 nm," *Opt. Lett.*, vol. 38, no. 4, pp. 501–503, 2013.

[10] T. Feng, D. Ding, F. Yan, Z. Zhao, H. Su, and X. S. Yao, "Widely tunable single-/dual-wavelength fiber lasers with ultra-narrow linewidth and high OSNR using high quality passive subring cavity and novel tuning method," *Opt. Exp.*, vol. 24, no. 17, pp. 19760–19768, 2016.

[11] Y. W. Song, S. A. Havstad, D. Starodubov, Y. Xie, A. E. Willner, and J. Feinberg, “40-nm-wide tunable fiber ring laser with single-mode operation using a highly stretchable FBG,” *IEEE Photon. Technol. Lett.*, vol. 13, no. 11, pp. 1167–1169, Nov. 2001.

[12] C. S. Kim, F. N. Farokhrooz, and J. U. Kang, “Electro-optic wavelength-tunable fiber ring laser based on cascaded composite Sagnac loop filters,” *Opt. Lett.*, vol. 29, no. 14, pp. 1677–1679, 2004.

[13] C. H. Yeh, T. T. Huang, H. C. Chien, C. H. Ko, and S. Chi, “Tunable S-band erbium-doped triple-ring laser with single-longitudinal-mode operation,” *Opt. Exp.*, vol. 15, no. 2, pp. 382–326, 2006.

[14] Y. Liu *et al.*, “Narrow line-width single-longitudinal-mode fiber laser using silicon-on-insulator based micro-ring-resonator,” *Laser Phys. Lett.*, vol. 13, no. 2, 2016, Art. no. 025102.

[15] S. Pan and J. Yao, “Frequency-switchable microwave generation based on a dual-wavelength single-longitudinal-mode fiber laser incorporating a high-finesse ring filter,” *Opt. Exp.*, vol. 17, no. 14, pp. 12167–12173, 2009.

[16] T. Wang, L. Zhang, C. Feng, M. Qin, and L. Zhan, “Tunable bistability in hybrid Brillouin–erbium single-frequency fiber laser with saturable absorber,” *J. Opt. Soc. Amer. B*, vol. 33, no. 8, pp. 1635–1639, 2016.

[17] R. N. Liu, I. A. Kostko, R. Kashyap, K. Wu, and P. Kiiveri, “Inband-pumped, broadband bleaching of absorption and refractive index changes in erbium-doped fiber,” *Opt. Commun.*, vol. 255, no. 1, pp. 65–71, 2005.

[18] L. Richter, H. Mandelberg, M. Kruger, and P. McGrath, “Linewidth determination from self-heterodyne measurements with subcoherence delay times,” *IEEE J. Quantum Electron.*, vol. QE-22, no. 11, pp. 2070–2074, Nov. 1986.

[19] H. Ludvigsen, M. Tossavainen, and M. Kaivola, “Laser linewidth measurements using self-homodyne detection with short delay,” *Opt. Commun.*, vol. 155, no. 1, pp. 180–186, 1998.

[20] Y. Zhao *et al.*, “Research on a novel composite structure Er 3+-doped DBR fiber laser with a π-phase shifted FBG,” *Opt. Exp.*, vol. 21, no. 19, pp. 22515–22522, 2013.

[21] W. J. Yue, Y. X. Wang, C. D. Xiong, Z. Y. Wang, and Q. Qiu, “Intensity noise of erbium-doped fiber laser based on full quantum theory,” *J. Opt. Soc. Amer. B*, vol. 30, no. 2, pp. 275–281, 2013.